GEOPHYSICAL RESEARCH LETTERS, VOL. 34, L23708, doi:10.1029/2007GL031601, 2007

Impact of the Atlantic Multidecadal Oscillation on North Pacific climate variability

Rong Zhang[1] and Thomas L. Delworth[1]

Received 6 August 2007; revised 4 October 2007; accepted 5 November 2007; published 12 December 2007.

[1] In this paper, we found that the Atlantic Multidecadal Oscillation (AMO) can contribute to the Pacific Decadal Oscillation (PDO), especially the component of the PDO that is linearly independent of El Niño and the Southern Oscillation (ENSO), i.e. the North Pacific Multidecadal Oscillation (NPMO), and the associated Pacific/North America (PNA) pattern. Using a hybrid version of the GFDL CM2.1 climate model, we show that the AMO provides a source of multidecadal variability to the North Pacific, and needs to be considered along with other forcings for North Pacific climate change. The lagged North Pacific response to the North Atlantic forcing is through atmospheric teleconnections and reinforced by oceanic dynamics and positive air-sea feedback over the North Pacific. The results indicate that a North Pacific regime shift, opposite to the 1976–77 shift, might occur now a decade after the switch of the observed AMO to a positive phase around 1995. **Citation:** Zhang, R., and T. L. Delworth (2007), Impact of the Atlantic Multidecadal Oscillation on North Pacific climate variability, *Geophys. Res. Lett.*, *34*, L23708, doi:10.1029/2007GL031601.

1. Introduction

[2] Large-scale climate variability in the North Pacific, such as the PDO, has been observed during the 20th century. The PDO index is defined as the leading principal component of North Pacific (poleward of 20°*N*, PC1_NP) sea surface temperature (SST) variability, and has both bidecadal and multidecadal time scales [*Mantua et al.*, 1997]. The transitions between PDO phases are often referred to as North Pacific climatic regime shifts, such as the shift occurred during 1976–77, as well as the shifts detected in the 1920s and 1940s. North Pacific climate variability has been linked to ENSO through the atmospheric bridge [*Lau and Nath*, 1994; *Deser and Blackmon*, 1995; *Zhang et al.*, 1996]. The leading Empirical Orthogonal Function of winter SST anomalies over the Pacific ocean (20°*S*–60°*N*, EOF1_Pacific) is dominated by ENSO at the interannual timescale [*Deser and Blackmon*, 1995]. However, the second EOF of Pacific winter SST anomalies (EOF2_Pacific), has been shown to be a North Pacific multidecadal mode linearly independent of ENSO [*Deser and Blackmon*, 1995; *Zhang et al.*, 1996]. Hereafter we refer to EOF2_Pacific as the North Pacific Multidecadal Oscillation (NPMO) and PC2_Pacific as the NPMO index, to emphasize its multidecadal feature. The SST signature of NPMO is confined mainly to the extratropical North Pacific. The corresponding winter 500-mb geopotential height signature resembles closely the PNA pattern [*Wallace and Gutzler*, 1981], i.e. opposite midtroposphere height anomalies over the Aleutian low and northwestern Canada. Over the North Pacific domain, EOF1_Pacific and the NPMO (EOF2_Pacific) account for similar amounts of variance [*Zhang et al.*, 1996]. The NPMO is equivalent to the PDO (EOF1_NP) if the ENSO projection is removed from the SST anomalies [*Zhang et al.*, 1996].

[3] Ocean dynamics has been suggested to play a very important role for the North Pacific decadal variability [*Latif and Barnett*, 1994; *Pierce et al.*, 2001]. However, the mechanism for the North Pacific *multidecadal* variability is still unclear. In particular, what physical processes are responsible for the *multidecadal* time scale of the NPMO? The Atlantic meridional overturning circulation (AMOC) is often considered one source of multidecadal variability in the Atlantic ocean. Multidecadal AMOC variability has been linked to the observed AMO index, which is definded as the detrended low-pass filtered annual mean SST anomalies averaged over the entire North Atlantic basin [*Enfield et al.*, 2001]. The observed large-scale AMO pattern resembles the simulated SST anomaly pattern induced by fluctuations of the AMOC [*Delworth and Mann*, 2000]. Can the AMO influence the North Pacific variability - such as the PDO? Paleo evidence suggests such a link. For example, higher oxygen levels off the California coast (indicating reduced upwelling and reduced California Current) were synchronous with Greenland cooling stadials [*Behl and Kennett*, 1996], that are in turn hypothesized to be linked to the AMOC weakening. Similarly, a link between changes in the North Pacific circulation and the AMOC is also seen in numerical experiments in which the AMOC is suppressed in response to massive fresh water inputs [*Zhang and Delworth*, 2005]. In this paper, using the GFDL hybrid coupled model (described below), we found that AMO-like fluctuations can contribute to the PDO and PNA pattern and induce the observed pattern of the NPMO, providing a source of multidecadal variability.

2. Comparing Modeled North Pacific Climate Variability With Observations

[4] We investigate the impact of the AMO on North Pacific Climate Variability by modifying the latest GFDL global coupled ocean-atmosphere model (CM2.1) [*Delworth et al.*, 2006] into a hybrid coupled model. Over the Atlantic basin only, we replace the fully dynamic ocean component of CM2.1 with a motionless slab ocean. The slab ocean interacts with the atmosphere only through exchanges of surface heat fluxes. Ocean basins outside the Atlantic

[1]Geophysical Fluid Dynamics Laboratory, NOAA, Princeton, New Jersey, USA.

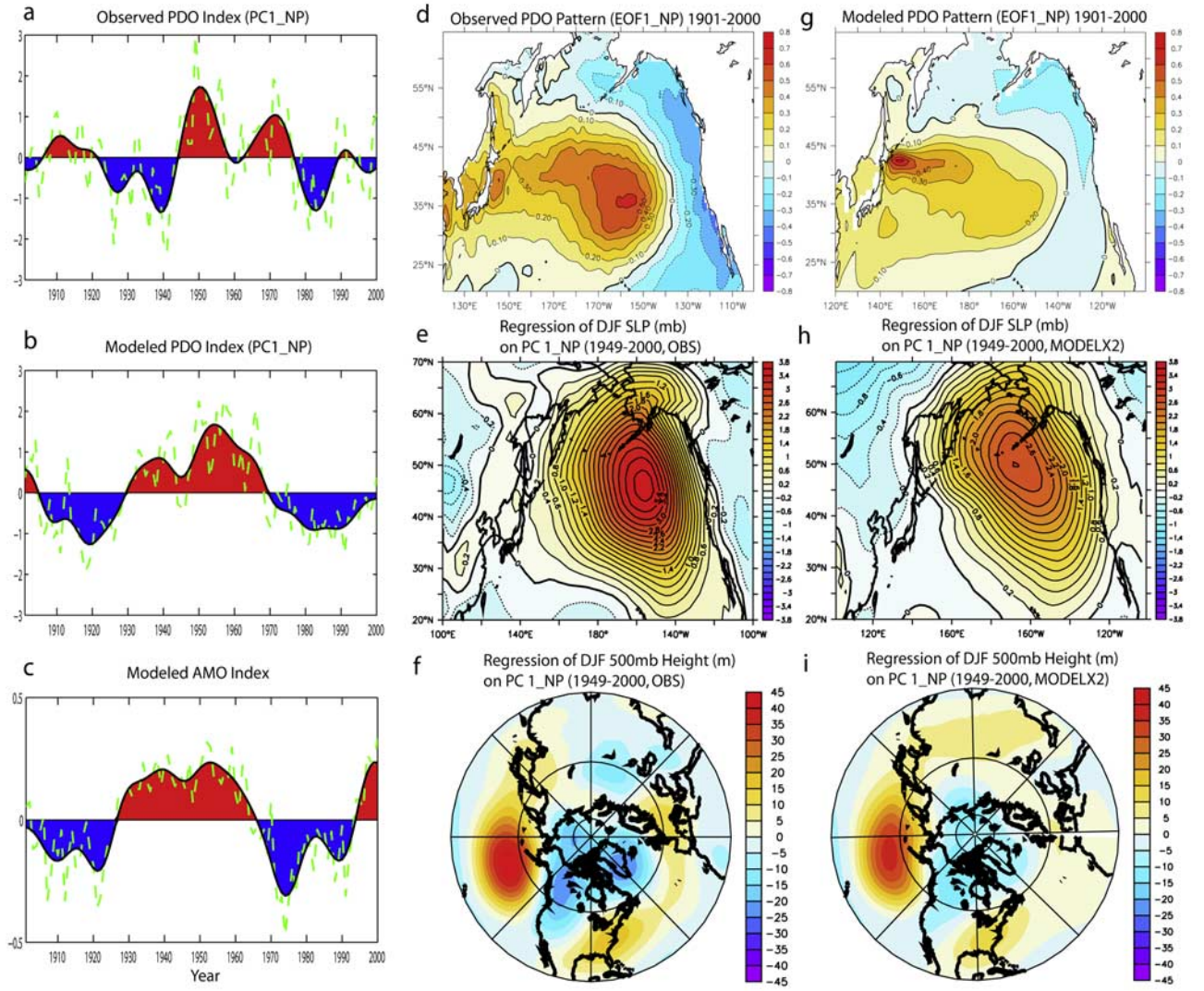

Figure 1. Observed and modeled PDO. (a, b) Observed and modeled PDO index PC1_NP. c, Modeled AMO Index. Color shading: low-pass filtered (LF) with a 10-year cutoff period; green dashed line: unfiltered. d, Observed PDO pattern - EOF1_NP. (e, f) Regressions of observed DJF SLP and 500-hPa height anomalies on observed PDO index. (g, h, i) same as (d, e, f) except using modeling results. (h, i) are scaled by a factor of 2.

remain fully dynamic in order to retain North Pacific climate variability as well as ENSO variability. A climatological heat flux is prescribed over the slab Atlantic so as to maintain observed seasonally varying SSTs. We further specified an anomalous heat flux that redistributes heat meridionally only within the Atlantic with zero spatial integral. The pattern of anomalous heat flux specified in the Atlantic is modulated by the observed low-pass filtered annual mean AMO Index (Supplementary Figure 1a[1]) from 1901 to 2000 to force the model to have AMO-like fluctuations over the Atlantic, equivalent to a time series of anomalous northward Atlantic ocean heat transport across the equator. An ensemble of 10 simulations is conducted for the 20th century. All results shown are ensemble means to reflect the Atlantic forced signal. In the slab North Atlantic, the simulated downward surface heat flux anomaly has almost the same magnitude and pattern (opposite sign) as the specified heat flux anomaly (Supplementary Figure 2). The simulated North Atlantic SST variability has similar magnitude and pattern as that observed (Supplementary Figure 3). The simulated AMO index (Figure 1c) has similar phase and amplitude as that observed (Supplementary Figure 1), thereby validating the experimental design as detailed in *Zhang and Delworth* [2006].

[5] To compare with the simulations, all observed data are detrended over the periods of comparison. All EOF analyses are performed for winter (DJF). Figures 1a and 1b compare the observed 20th century PDO index (PC1_NP) derived from HADISST dataset [*Rayner et al.*, 2003] with that simultated. The observed PDO pattern, i.e. EOF1 of the North Pacific DJF SST anomalies (EOF1_NP) (corresponding to a positive PDO phase, Figure 1d), is characterized by a horseshoe pattern of warm SST anomalies in the central/western North Pacific and cold SST anomalies off the west

[1]Auxiliary materials are available in the HTML. doi:10.1029/2007GL031601.

coast of North America. Note here the sign of the PDO index and pattern (Figure 1) are opposite to the convention [*Mantua et al.*, 1997], i.e. we choose to have the positive PDO index represent warming over the central and western North Pacific, not warming over the tropical eastern Pacific. The observed DJF atmospheric signatures associated with the positive PDO phase (derived from NCEP-NCAR reanalysis [*Kistler et al.*, 2001] for the period of 1949–2000) show anomalous high SLP and 500-mb height south of the Aleutian Islands and anomalous low 500-mb height over northwestern Canada (Figures 1e and 1f); we refer to this as the positive PNA pattern here (again the sign is opposite to the convention for the PNA [*Wallace and Gutzler*, 1981]).

[6] The simulated PDO (Figure 1g) also shows the horseshoe pattern, but the SST signature is stronger in the western North Pacific and weaker in the central and eastern North Pacific. The simulated corresponding atmospheric signatures (Figures 1h and 1i, scaled by a factor of 2) also exhibit a positive PNA pattern as observed (Figures 1e and 1f), but with much weaker amplitudes, probably due to the weaker SST signature over the central North Pacific, weaker atmospheric responses to the North Pacific SST anomalies, and ensemble average in the model. Both the observed and simulated PDO index (Figures 1a and 1b) show multidecadal variability. The simulated unfiltered PDO index lags the simulated unfiltered AMO index by 3 years at the maximum correlation r = 0.66, significant at the 95% level with an effective degree of freedom (dof) of 9 (Figures 1b and 1c). The effective dof is the sample size divided by the decorrelation time between these two variables. The observed unfiltered PDO index (Figure 1a) lags the observed unfiltered AMO index by 12 years at the maximum correlation r = 0.47, significant at the 99% level with an effective dof of 28. For example, the observed central and western North Pacific SST switches from a warming phase to a cooling phase during 1976–77 (Figure 1a). The simulated one has similar shift around 1970 (Figure 1b), following the switch of the AMO index from a positive phase to a negative phase around 1965 (Figure 1c).

[7] The PDO consists of both the projection of ENSO onto the North Pacific as well as North Pacific variability that is independent from ENSO. In this paper, we focus on the latter part. To separate the North Pacific variability from the ENSO projection, EOF analyses are performed for winter (DJF) over the Pacific ($20^{\circ}S$–$60^{\circ}N$) including the tropical region. The observed EOF1_Pacific shows the ENSO signal and its projection over the central and eastern North Pacific (Figure 2e). The simulated EOF1_Pacific also shows the ENSO signal in the tropical eastern Pacific, but its contribution to the North Pacific is much weaker (Figure 2f). The observed and simulated PC1_Pacific both exhibit more interannual fluctuations and can be viewed as the ENSO index. The observed EOF2_Pacific, i.e. NPMO, is orthogonal to EOF1_Pacific and thus linearly independent of EOF1_Pacific, and the maximum SST signature is in the western midlatitudes (Figure 2g), similar to that shown in previous studies [*Deser and Blackmon*, 1995; *Zhang et al.*, 1996]. The simulated NPMO (EOF2_Pacific) shows very similar pattern as observed, i.e. a horseshoe pattern in the North Pacific with the maximum SST signature confined to the western midlatitudes, and not much signal in the tropical eastern Pacific (Figure 2h). The observed and simulated PC2_Pacific, i.e. the NPMO index, are both dominated by multidecadal variability (Figures 2c and 2d).

[8] The observed and simulated height anomalies associated with the ENSO signal (Figures 2i and 2j, reversed sign) both show more zonally symmetric feature with the positive height anomalies over the central North Pacific extended eastward to the U.S. continent. Both observed and simulated heights anomalies associated with the NPMO (Figures 2k and 2l) resemble more closely the positive PNA pattern, i.e. the negative height anomalies over the northwestern Canada extend southward to the western U.S. and eastern North Pacific. The simulated atmospheric signatures (Figures 2j and 2l, scaled by a factor of 2) are also much weaker than that observed (Figure 2i and 2k), probably due to weaker atmospheric responses to SST anomalies and ensemble average in the model. The simulated unfiltered PC2_Pacific (the unfiltered NPMO index) lags the simulated unfiltered AMO index by 2 years at the maximum correlation r = 0.71, significant at the 98% level with an effective dof of 9 (Figure 2d and Figure 1c). The observed unfiltered NPMO index (Figure 2c) lags the observed unfiltered AMO index by 13 years at the maximum correlation r = 0.38, significant at the 95% level with an effective dof of 30. The modeling results suggest that the AMO can contribute to the component of the PDO that is linearly independent of ENSO, i.e. the NPMO, and the associated PNA pattern.

[9] How does the North Atlantic-North Pacific teleconnection occur and what affects the time lag between the PDO and the AMO? Here we propose a mechanism (Figure 3) for the influence of the AMO on the North Pacific multidecadal variability:

[10] 1. During the positive (negative) AMO phase, the warm (cold) North Atlantic SST anomaly leads to reduced (enhanced) surface DJF northward atmospheric eddy heat transport and upper level DJF eddy vorticity flux over both the North Atlantic and the North Pacific mid-latitudes (Supplementary Figure 6), in response to the enhanced northward oceanic heat transport. This weakening (strengthening) of the mid-latitude winter storm track results in a poleward (equatorward) shift of the westerly wind, and thus the weakening (strengthening) of the Aleutian Low, i.e. high (low) SLP anomaly and positive (negative) PNA pattern over the North Pacific.

[11] 2. The negative (positive) wind stress curl anomaly associated with the high (low) SLP anomaly over the North Pacific leads to an anomalous anticyclonic (cyclonic) midlatitude gyre circulation (Supplementary Figure 7), and thus a northward (southward) shift of the Kuroshio Current and warm (cold) SST anomaly in the central and western North Pacific, especially near the Kuroshio/Oyashio Extension (KOE) region. Observational analysis [*Miller and Schneider*, 2000] shows that the warm (cold) KOE SST anomaly is a gyre-scale response to wind stress curl forcing associated with the North Pacific high (low) SLP anomaly, and lags the central North Pacific signal by about 5 years, a time scale for Rossby wave propagation from the central North Pacific to the KOE region. Our modeled KOE SST anomaly lags modeled central North Pacific signal by about 4 years, consistent with observations and the previous modeling study [*Seager et al.*, 2001]. Our modeled unfil-

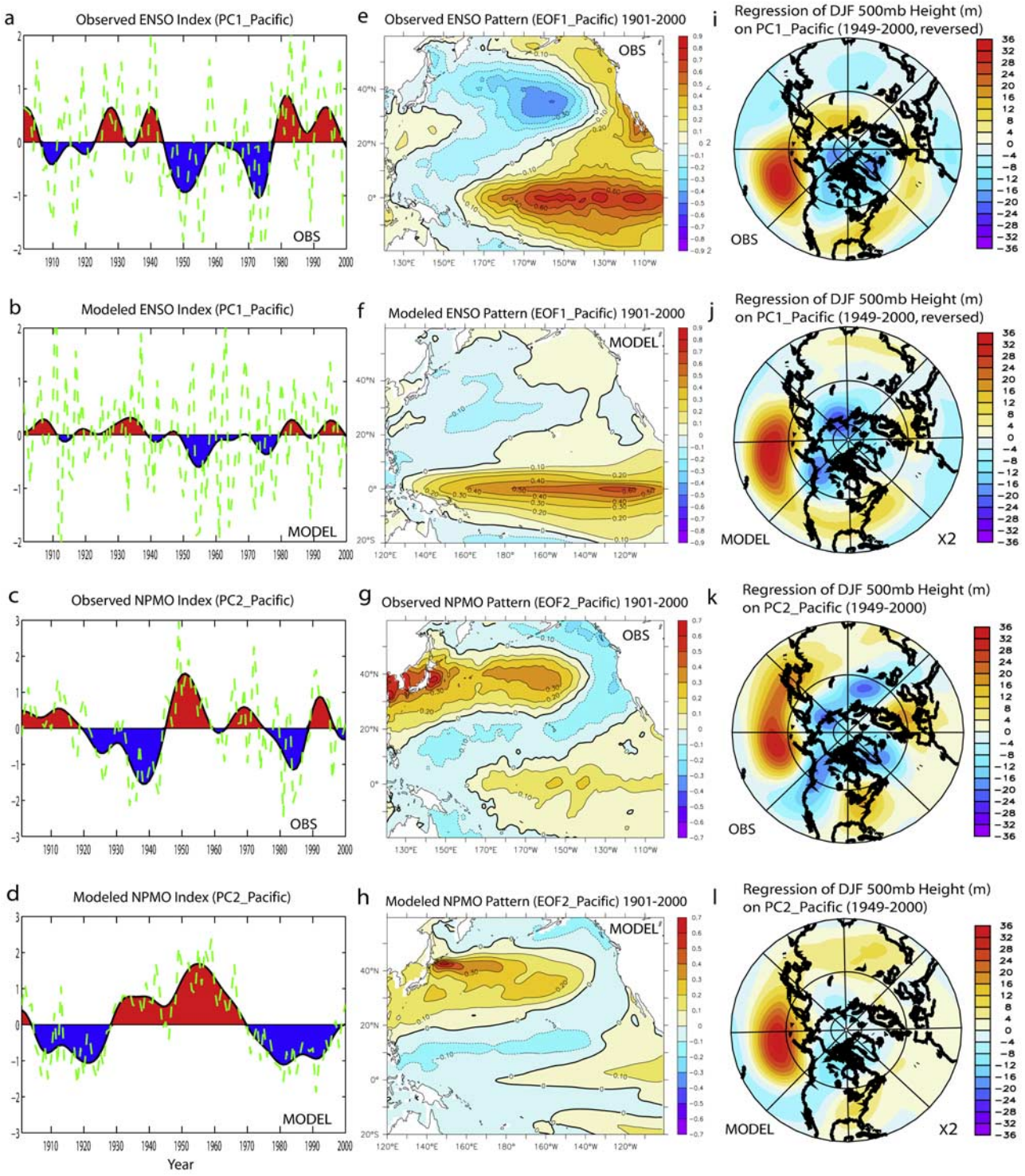

Figure 2. Observed and modeled ENSO and NPMO. (a, c) Observed PC1_Pacific and PC2_Pacific. (e, g), Observed EOF1_Pacific and EOF2_Pacific. (i, k) Regressions of observed DJF 500-hPa height anomalies on observed PC1_Pacific and PC2_Pacific. The sign in (i) is reversed for comparison with (k). (b, d, f, h, j, l) same as (a, c, e, g, i, k) except using modeling results. (j, l) are scaled by a factor of 2.

tered KOE SST anomaly lags modeled unfiltered AMO Index by about 7 years (Figure 3b) at the maximum correlation (r = 0.63), significant at the 95% level with an effective dof of 10. Similar lag correlation also exists in a 1000-year control simulation using the latest GFDL global fully coupled model (CM2.1), in which the KOE SST anomaly lags the AMO index by 5–7 years at the maximum correlation (r = 0.6), significant at the 99% level with an effective dof of 23 (Supplementary Figure 8). The AMO signal in the CM2.1 control simulation is induced by the

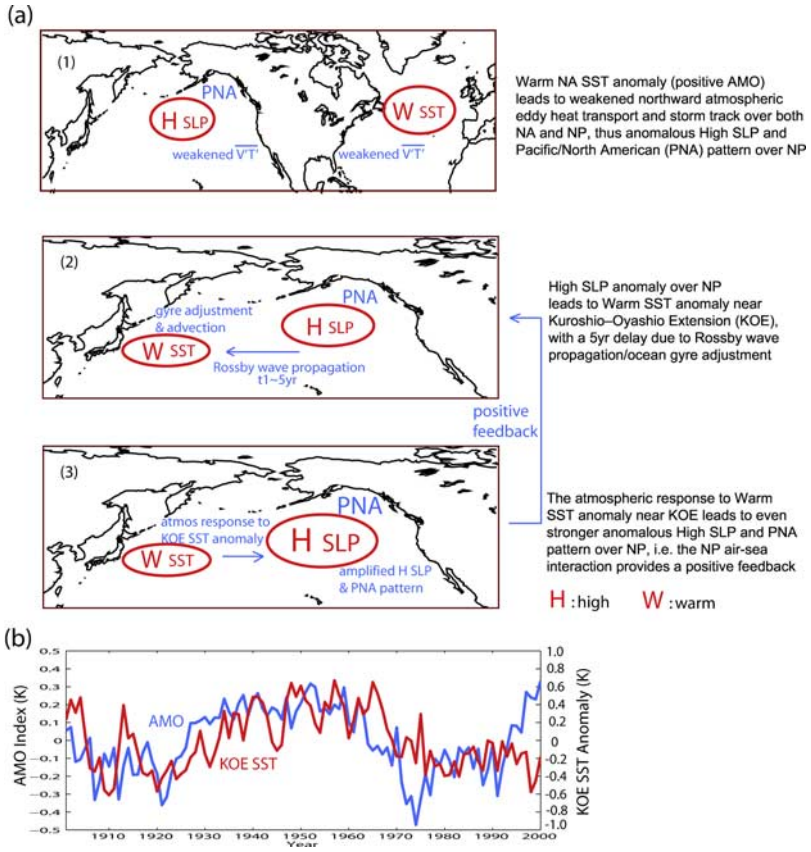

Figure 3. (a) Schematic diagram of the hypothesized mechanism. (b) Modeled AMO Index and DJF KOE (130°–160°*E*, 38°–45°*N*) SST anomaly (unfiltered).

AMOC variability with a timescale of about 250 years, and thus the anomalies are low-pass filtered with a 50-year cutoff period.

[12] 3. The atmospheric response to the warm (cold) SST anomaly in the KOE region leads to even stronger weakening (strengthening) of the Aleutian Low, i.e. amplified high (low) SLP anomaly and positive (negative) PNA pattern over the North Pacific. Hence the North Pacific air-sea interaction provides a positive feedback and the excited North Pacific multidecadal mode can persist. In a previous study [*Zhang and Delworth*, 2005], when the same atmospheric model is coupled to a global slab ocean, and a similar amount of anomalous heatflux (induced by the weakening of the AMOC) as that obtained with the fully coupled model is prescribed over the Atlantic, the resulting KOE SST anomaly [*Zhang and Delworth*, 2005] and associated PNA pattern are much weaker than that in the fully coupled model (Supplementary Figure 9). This suggests that the PNA pattern can be amplified through its response to the KOE SST anomaly and indicates a positive air-sea feedback.

[13] The lag between the KOE SST anomaly and the AMO index is mainly affected by the Rossby wave propagation time scale in the North Pacific (t1 ≈ 5 years) and the strength of the positive feedback. With a stronger positive feedback, the KOE SST anomaly would be less damped and would persist longer. This process would lead to a longer phase delay between the AMO and PDO than occurs in our model by countering the tendency to flip the phase of the PDO that is induced by a switch in sign of the AMO. Our simulated North Pacific atmospheric response to SST anomalies and the associated positive feedback may be too weak, contributing to the much shorter time lag of the PDO to the AMO index than observed. The KOE SST anomaly is an important signature of the NPMO. Our modeled ENSO projection over the North Pacific is much weaker than observed (Figures 2e and 2f). Hence the modeled PDO is strongly affected by the NPMO, and the simulated PDO index is very similar to the simulated NPMO index (Figure 1b and Figure 2d). The phase of the PDO/NPMO Index is close to the phase of the central North Pacific signal, thus the lag between the PDO/NPMO and the AMO index is shorter than the lag between the KOE SST anomaly and the AMO index, because the KOE SST anomaly lags the central North pacific signal by about 4 years. The central North Pacific signal is the sum of the response to the AMO signal, and the response to KOE SST anomalies which lag the AMO for years. The lag between the central North Pacific signal and the AMO is affected by amplitudes of these two responses. Thus the stronger the positive feedback is, the longer the lag. In reality, the low frequency variability of ENSO also contributes to the PDO.

[14] *Latif and Barnett* [1994] suggest that a warm (cold) KOE SST anomaly leads to a high (low) SLP anomaly over the North Pacific, consistent with part (3) of our proposed mechanism; but they also proposed that the high (low) SLP anomaly over the North Pacific will eventually lead to a cold (warm) KOE SST anomaly, opposite to both part (2) of our proposed mechanism and observations [*Miller and*

Schneider, 2000]. Hence they proposed a negative feedback (warm KOE SST → high SLP → cold KOE SST) that is necessary to flip the phase and generate internal North Pacific decadal oscillations. Here we propose a positive feedback (warm KOE SST → high SLP → warm KOE SST) when combining part (2) and (3) of the mechanism, and the flipping of the phase at multidecadal time scales is forced remotely by the AMO.

3. Conclusion and Discussion

[15] The simulated ensemble mean suppresses internally generated North Pacific variability and ENSO teleconnections, but shows the Atlantic forced North Pacific multidecadal variability. The results suggest the AMO can contribute to the PDO, especially the component of the PDO that is linearly independent of ENSO, i.e. the NPMO, and the associated PNA pattern. The simulated time lag between the unfiltered PDO and AMO (3 years) is much shorter than that observed (12 years), probably due to relatively weak North Pacific air-sea interactions in the model. The results indicate that a regime shift of the North Pacific climate to a phase of warming over the central and western North Pacific and cooling off the west coast of the North America, opposite to the 1976–77 shift, might occur now in the early 21st century, a decade after the switch of the observed AMO to a positive phase at about 1995. The AMO might serve as one of the sources or triggers of North Pacific multidecadal variability.

[16] Our hypothesized mechanism needs to be verified by future modeling and observational studies. In particular, various previous studies show conflicting results regarding part (3) of the mechanism. Our simulated maximum SST anomalies are confined to the KOE region and do not spread eastward, indicating the model's deficiency in advecting KOE SST anomalies by the Kuroshio Current, a typical problem with coarse resolution ocean models [*Pierce et al.*, 2001]. Observational analyses show a 10-year time scale for advecting the SST anomalies just off Japan eastward to the dateline to affect the atmosphere [*Pierce et al.*, 2001]. This decadal advection time scale introduces an additional lag, which is missing in our coarse resolution model, and might contribute to the much longer lag between the observed PDO/NPMO and AMO. We also suspect that the model's atmospheric response over the central North Pacific may be too weak.

[17] The difference between simulated and observed PDO/NPMO indices reflects the deficiency in simulating the proper time lag relative to the AMO, and also indicates that other factors may play a role. Recent coupled model results [*Latif*, 2006] suggest that the North Pacific multidecadal variability evolves largely independently of the variations in the tropical Pacific, and can be explained by the dynamical ocean response to stochastic wind stress forcing. Future experiments might be designed to isolate the pure impact of stochastic forcing on the North Pacific multidecadal variability by suppressing the AMO signal in the coupled model.

References

Behl, R., and J. P. Kennett (1996), Brief interstadial events in the Santa Barbara basin, NE Pacific, during the past 60 kyr, *Nature*, *379*, 243–246.

Delworth, T. L., and M. E. Mann (2000), Observed and simulated multidecadal variability in the Northern Hemisphere, *Clim. Dyn.*, *16*, 661–676.

Delworth, T. L., et al. (2006), GFDL's CM2 global coupled climate models. Part I: Formulation and simulation characteristics, *J. Clim.*, *19*, 643–674.

Deser, C., and M. L. Blackmon (1995), On the relationship between tropical and North Pacific sea surface temperature variations., *J. Clim.*, *8*, 1677–1680.

Enfield, D. B., A. M. Mestas-Nuñez, and P. J. Trimble (2001), The Atlantic multidecadal oscillation and its relation to rainfall and river flows in the continental U.S., *Geophys. Res. Lett.*, *28*, 2077–2080.

Kistler, R., et al. (2001), The NCEP-NCAR 50-year reanalysis: Monthly means CD-ROM and documentation, *Bull. Am. Meteorol. Soc.*, *82*, 247–268.

Latif, M. (2006), On North Pacific multidecadal climate variability, *J. Clim.*, *19*, 2906–2915.

Latif, M., and T. P. Barnett (1994), Causes of decadal climate variability over the North Pacific/North American sector, *Science*, *226*, 634–637.

Lau, N.-C., and M. J. Nath (1994), A modeling study of the relative roles of tropical and extratropical SST anomalies in the variability of the global atmosphere-ocean system, *J. Clim.*, *7*, 1184–1207.

Mantua, N. J., S. R. Hare, Y. Zhang, J. M. Wallace, and R. C. Francis (1997), A Pacific interdecadal climate oscillation with impacts on salmon production, *Bull. Am. Meteorol. Soc.*, *78*, 1069–1079.

Miller, A. J., and N. Schneider (2000), Interdecadal climate regime dynamics in the North Pacific Ocean: Theories, observations, and ecosystem impacts, *Progr. Oceanogr.*, *47*, 355–379.

Pierce, D. W., T. P. Barnett, N. Schneider, R. Saravanan, D. Dommenget, and M. Latif (2001), The role of ocean dynamics in producing decadal climate variability in the North Pacific, *Clim. Dyn.*, *18*, 51–70.

Rayner, N. A., et al. (2003), Global analyses of sea surface temperature, sea ice, and night marine air temperature since the late nineteenth century, *J. Geophys. Res.*, *108*(D14), 4407, doi:10.1029/2002JD002670.

Seager, R., Y. Kushnir, N. H. Naik, M. A. Cane, and J. Miller (2001), Wind-driven shifts in the latitude of the Kuroshio-Oyashio Extension and generation of SST anomalies on decadal timescales, *J. Clim.*, *14*, 4249–4265.

Wallace, J. M., and D. S. Gutzler (1981), Teleconnections in the geopotential height field during the Northern Hemisphere winter, *Mon. Weather Rev.*, *109*, 784–812.

Zhang, R., and T. L. Delworth (2005), Simulated tropical response to a substantial weakening of the Atlantic thermohaline circulation, *J. Clim.*, *18*, 1853–1860.

Zhang, R., and T. L. Delworth (2006), Impact of Atlantic Multidecadal Oscillations on India/Sahel Rainfall and Atlantic Hurricanes, *Geophys. Res. Lett.*, *33*, L17712, doi:10.1029/2006GL026267.

Zhang, Y., J. M. Wallace, and N. Iwasaka (1996), Is Climate Variability over the North Pacific a Linear Response to ENSO?, *J. Clim.*, *9*, 1468–1478.

T. L. Delworth and R. Zhang, Geophysical Fluid Dynamics Laboratory, NOAA, Princeton, NJ, 08540, USA. (rong.zhang@noaa.gov)